ELSEVIER

International Journal of Mass Spectrometry 213 (2002) 191–202

www.elsevier.com/locate/ijms

Evaluation of micro-electrospray ionization with ion mobility spectrometry/mass spectrometry

Laura M. Matz, Wes E. Steiner, Brian H. Clowers, Herbert H. Hill, Jr

Washington State University, Chemistry Department, Pullman, Washington 99164-4630

Received 25 June 2001; accepted 26 September 2001

Abstract

In recent years, the resolving power of ion mobility instruments has been increased significantly, enabling ion mobility spectrometry (IMS) to be utilized as an analytical separation technique for complex mixtures. In theory, decreasing the drift tube temperature results in increased resolution due to decreased ion diffusion. However, the heat requirements for complete ion desolvation with electrospray ionization (ESI) have limited the reduction of temperatures in atmospheric pressure ion mobility instruments. Micro-electrospray conditions were investigated in this study to enable more efficient droplet formation and ionization with the objective of reducing drift tube temperatures and increasing IMS resolution. For small molecules (peptides), the drift tube temperature was reduced to ambient temperature with good resolution by employing reduced capillary diameters and flow rates. By employing micro-spray conditions, experimental resolution values approaching theoretically predicted resolution were achieved over a wide temperature range (30 to 250 °C). The historical heat requirements of atmospheric pressure IMS due to ESI desolvation were eliminated due to the use of micro-spray conditions and the high-resolution IMS spectra of GLY-HIS-LYS was obtained at ambient temperature. The desolvation of proteins (cytochrome c) was found to achieve optimal resolution at temperatures greater than 125 °C. This is significantly improved from earlier IMS studies that required drift tube temperatures of 250°C for protein desolvation. (Int J Mass Spectrom 213 (2002) 191–202)

1. Introduction

Atmospheric pressure ion mobility spectrometry (IMS) has been employed for over thirty years [1] and has made significant contributions to the detection of many volatile organic compounds [1]. However, the separations applicable for IMS have been limited due to the low resolution of the instrument and the limitations imposed by traditional ionization methods, which required analytes to be volatile.

The ionization limitations of IMS were eliminated with the introduction of electrospray ionization (ESI) as an ionization source for IMS instruments [2–7]. Dole and coworkers first showed the electrospray of lysozyme with an IMS instrument in 1972, which produced three broad peaks [2]. In 1977, further experiments by Dole et al. to electrospray polystyrene oligomers found the formation of several broad peaks and the group speculated that the broad peaks were due to excess solvent ions [3]. After these two early works, the group concluded that the solvent evaporation would be difficult without entry into a vacuum chamber and that ESI was limited to mass spectro-

* Corresponding author. E-mail: Hhhill@wsu.edu

1387-3806/02/$22.00
PII S1387-3806(01)00534-6

metry (MS). In these experiments, the drift gas was flowing in the same direction as the ion migration. Improvements in 1987 by Shumate and Hill were made to the ESI/IMS design by employing a counterflow of heated drift gas that served to completely desolvate the ions [4]. Using this approach, the first mobilities of a number of nonvolatile and high molecular weight compounds were measured. However, this ESI design was unable to electrospray high molecular weight compounds (proteins) and was susceptible to corona discharge due to heating of the ESI source caused by the heated drift gas. Further experiments in 1991 by Smith et al. produced similar results to Dole's early experiments for proteins and the evidence of multiply charged ions characteristic of ESI in MS was still unproven [5]. In 1994, our lab showed that with a counterflow of heated drift gas and a water-cooled electrospray needle, the ESI/IMS spectra of cytochrome c (12kDa protein) was possible [6]. The separation of multiple charges on cytochrome c was observed along with oligomer separations and this work finally proved the potential of ESI as an ionization method for IMS. In 1995, Clemmer et al. showed the first mass selected mobilities for cytochrome c [7]. This work exhibited the first example of an ion mobility separation of multiple protein conformers for a single charge state. Further work in 1997 by McCooey et al. employed a capillary interface between the ESI and atmospheric pressure IMS [8] and a similar temperature dependence was observed for the resolution of cytochrome c charge states.

Since ESI and matrix assisted laser desorption ionization (MALDI) sources were interfaced to IMS instruments, the field of IMS for a wide range of biological applications has increased substantially including drugs [9], chemical warfare agents [10], peptides [11,12], and proteins [6,8,13,14] (see extensive reviews in [15]). Much of the work performed on proteins and peptides has been performed with reduced pressure systems (~1–10 Torr [11b] or higher pressure systems at ~100–200 Torr [11a,12d,13a]). Due to the entry of ESI ions into a reduced pressure region prior to entering the drift tube, solvent molecules are removed in the interface region [16,17]. In contrast, drift tubes operated at atmospheric pressure require substantial heating in order to remove all solvent molecules prior to the mobility experiment [6,8,14]. Therefore, atmospheric pressure IMS systems have required operation at elevated temperatures to ensure ion desolvation [14], but reduced pressure systems are typically operated at ambient temperature [11b].

Resolution, in IMS, is typically reported as resolving power (Rp) and measured for a single peak according to the following equation [18]:

$$R_p = \frac{t_d}{w_h} \tag{1}$$

where t_d is the ion's drift time (milliseconds) and w_h is the peak width at half height. Dependent on the context, the resolving power or separation efficiency can also be reported in chromatographic terms (theoretical plates, N) as shown below [19]:

$$N = 5.55\left(\frac{t_d}{w_h}\right)^2 = 5.55R_p^2 \tag{2}$$

Revercomb and Mason derived a relationship for the peak width which accounted for contributions only from the initial pulse width (t_g) and the broadening due to diffusion [20]:

$$w_h^2 = t_g^2 + \left(\frac{16kT\ \ln 2}{Vez}\right)t_d^2 \tag{3}$$

where w_h is the peak width at half height, k is Boltzman's constant, T is the temperature (K), V is the voltage drop across the drift region, e is the elementary charge, and z is the number of charges on the ion. This equation does not account for peak broadening due to Coulombic repulsion and electric field inhomogeneity.

The diffusion limited resolving power is defined as the maximal theoretical resolving power an instrument can attain. The limit occurs when t_d becomes very large compared to t_g and is determined based on the following equation

$$R_d \equiv \lim R\left(\frac{t_g}{t_d} \rightarrow 0\right) = \left(\frac{Vez}{16kT\ \ln 2}\right)^{1/2} = 0.300\left(\frac{Vez}{kT}\right)^{1/2} \tag{4}$$

Several labs have reported significant increases in resolving power by interfacing IMS instruments with an MS [12,21,19]. Our lab recently reported a high resolution IMS/MS instrument that achieved resolutions comparable to the theoretically predicted maximum [14]. Due to sampling from the drift tube center, the resolving power was thought to be independent of broadening contributions from Coulombic repulsion and electric field inhomogeneity and the reason for the considerably higher resolving power achieved.

Eq. (3) shows that several experimental parameters affect the resolving power obtained in IMS. In order to decrease w_h (and consequently increase R_p), a researcher can; (1) decrease the gate width, (2) increase the voltage drop across the drift region (with an increase in the drift length to achieve similar drift times), (3) increase the number of charges, and (4) decrease the temperature. Further improvements in IMS resolving power have been reported by several groups by evaluating increases in voltage (with subsequent increase in drift length) [19,21,22]. Dugourd et al. used a 63 cm long drift tube to achieve resolving powers up to 172 (164 000 theoretical plates) [21]. The increase in drift length (22.5 cm) and voltage for our high-resolution instrument increased regularly achieved resolving powers (reported as theoretical plates) to 150 (125 000 theoretical plates) [11]. Srebalus et al. reported resolving powers up to 260 (375 000 theoretical plates) for ions with 4 charges using their high-resolution instrument [23] and our lab reported R_p values of up to 216 for multiply charged ions [14]. Recently, Collins and Lee reported the operation of an ambient temperature IMS instrument that achieved resolution values of 76 [24]. The use of a new desolvation ring design, along with a 27 cm drift region, enabled their IMS instrument to achieve higher resolving powers than attained with conventional ESI/IMS instruments.

In atmospheric pressure IMS drift tubes, temperatures have not been decreased (to further improve resolution) due to the temperature requirements for ion desolvation in ESI. The use of smaller capillary diameters in ESI/MS literature with accompanying smaller flow rates, labeled microelectrospray [25,26] and nanospray [27,28], have been shown to provide more efficient droplet formation and ionization. ESI/MS studies have shown that lower flow rates and smaller inner capillary diameters provide smaller Taylor cone formation and produce smaller droplets [29]. By employing microelectrospray conditions in our ESI/IMS/MS system, it was hypothesized that the droplet sizes would be smaller and hence, require less thermal energy (lower drift tube temperatures) for complete ion desolvation. The ability to decrease the drift tube temperature without compromising ESI desolvation would enable higher resolution separations [as shown in Eq. (3)].

In this paper, we investigate the use of microelectrospray ionization with IMS/MS. The effect of the smaller diameter capillaries on resolving power was evaluated for temperatures down to approximately ambient temperature. The effect of temperature and capillary size were evaluated for both a small peptide and cytochrome c.

2. Experimental

2.1. Instrumentation

The ESI/IMS/MS instrument that was utilized for all experiments was constructed at Washington State University. A water-cooled ESI source was utilized for all experiments and has been described previously [6]. The IMS/MS instrument was discussed in the literature [14] and recent modifications to the instrument have been further documented [11].

The IMS instrument consisted of two regions; a desolvation region (7.2 cm in length) and a drift region (22.5cm in length). The resistor size on the desolvation region was reduced from 1 MΩ to 500 kΩ in order to utilize more of the voltage on the drift region. The IMS was operated at 9.5 kV (7.9 kV at the ion gate) for all experiments. Nitrogen was employed as the drift gas and was operated at 1.1 L/min. The IMS was connected to a quadrupole MS via a 40 μm pinhole. The MS system had a mass range of 0–4000 amu and was purchased from ABB Extrel (Pittsburgh, PA, Model 150-QC). There were six lenses between the IMS and the quadrupole and the voltages were as

follows: +8.0 V (pinhole), −42.8 V (screen), −116.3 V (first einzel element), −34.5 V (second einzel element), −17.3 V (third einzel element), and −50.9 V (ELFS plate). The electron multiplier was operated at 1.7 kV for the solvent spectra and 1.9 kV for the analyte spectra (both the peptide and cytochrome c). In all cases, the dynode was operated at −5.0 kV and the quadrupole rods were biased at −20.8 V.

IMS data acquisition was performed with a Labview (National Instruments, Houston, TX) data acquisition card and Labview 5.0 software, which was modified at Washington State University. The gating electronics were controlled by the Labview software and the electronics have been described previously [6].

Three modes of instrument operation were employed in these experiments; mass spectra, nonselective ion mobility (NSIM) and selective ion monitoring (SIM). For mass spectra evaluation, the quadrupole was scanned while the IMS gate was left open and all ions were allowed to traverse the drift tube. For NSIM, the quadrupole direct current (dc) voltage (rf-only mode) was turned off while continually gating the ion mobility instrument. In this mode, ion mobility spectra were detected for all ions and the quadrupole simply transmitted the ions to be detected by the electron multiplier. In SIM mode, the ion mobility experiment was continually gated but only one *m/z* value was transmitted through the quadrupole and detected. In this mode, ion mobility spectra were obtained for ions with the designated *m/z* value.

2.2. Electrospray conditions

The electrospray solvent used was composed of 47.5% water/47.5% methanol with 5% acetic acid. A Harvard Apparatus (Holliston, MA) dual syringe pump equipped with a 250 μL Hamilton (Reno, NV) syringe was employed for all experiments. The electrospray needle was maintained at 12.0 kV, resulting in a difference of 3.5 kV between the needle and the target screen (first ring of the drift region).

2.3. Reagents and chemicals

A small 3-amino acid peptide (Glysine-Histidine-Lysine) was obtained from Sigma (St. Louis, MO) and was employed for all capillary evaluations (10^{-4} M range). The peptide was used at a high concentration level in order to ensure that the same solution concentration could be evaluated at all temperatures and capillary sizes. Cytochrome C was also obtained from Aldrich and used at the 10^{-4}M concentration level. The electrospray solvents were all reagent graded and obtained from J.T. Baker (Phillipsburg, NJ).

2.4. General experimental protocol

Three fused silica capillaries from PolyMicro Technologies (Phoenix, AZ) were used to evaluate the effect of inner diameter (i.d.) on IMS resolution; 100 μm i.d., 50 μm i.d., and 30 μm i.d. The capillary was placed approximately 1mm out of the metal ESI needle and placed approximately 2 mm away from the target screen, although these parameters were optimized for maximum signal intensity each time the capillary was changed. Both the desolvation region and drift tube temperature were varied in 25 °C increments from 30 °C to 250 °C, and at each temperature, the drift tube was allowed to equilibrate for one hour prior to experiments. The temperature studies were begun at 30 °C in order to determine any negative effects of working at lower temperatures. At each capillary size and temperature, the flow rate was varied between 5.0 and 0.60 μL/min (increments: 5.0, 3.0, 1.0, 0.8, and 0.6 μL/min).

The three capillary sizes and temperatures were evaluated by measuring the peptide response. For the peptide experiments, the scan time was 50 ms, except at 30 °C where the scan time was increased to 70 ms (due to the increasing drift time). For experimental resolution points, the calculations were performed based on Eq. (1). The theoretical resolution graphs (based on the operating conditions utilized in this study) (in Fig. 5) were calculated based on Eq. (3). The diffusion limited resolving power (in Fig. 5) was calculated according to Eq. (4). The MS was operated

Table 1
Percentage of *m/z* values observed in mass spectra at varied temperatures; Mass spectra were obtained for 100 μm capillary column at a flow rate of 1 μl/min

m/z	Ion identity	50 °C	100 °C	150 °C	200 °C	250 °C
37	$(H_2O)_2H^+$	23%	24%	15%		
55	$(H_2O)_3H^+$	100%	100%			
61	$(CH_3COOH)H^+$			37%		10%
73	$(H_2O)_4H^+$	91%	24%			20%
83	$(CH_3COOH)Na^+$	58%	45%	37%		20%
91	$(H_2O)_5H^+$	46%				
103				37%		20%
121	Contaminant			100%		20%
146	Contaminant			37%	21%	20%
192	Contaminant				100%	100%

in SIM mode so only the protonated peptide ion (*m/z* = 340) was detected. Along with peptide data, IMS solvent spectra and MS solvent spectra were obtained in order to evaluate any changes in the electrospray process due to temperature and/or capillary size. For cytochrome c experiments, the scan time was 100 ms for all temperatures and the graphs were typically the result of 5000 averages.

2.5. Calculations

All reduced mobility constants (K_o) and collision cross section (Ω) values were calculated from experimentally determined drift times (t_d). The reduced mobility constants were calculated according to [1]

$$K_o = \left(\frac{L^2}{V^* t_d}\right)\left(\frac{273}{T}\right)\left(\frac{P}{760}\right) \quad (5)$$

where L is the drift region length (22.5 cm), V is the drift voltage (7 900 V), T is the effective temperature in the drift region (523 K), and P is the pressure in the drift region (695–700 Torr).

The average ion collision cross section (Ω) was calculated from [20]

$$\Omega = \left(\frac{3}{16N}\right)\left(\frac{2\pi}{\mu kT}\right)^{1/2}\left(\frac{zeVt_d}{L^2}\right) \quad (6)$$

where z is the number of the charges on the ion, e is the charge of one proton, N is the number density of the drift gas, μ [= mM/(m + M)] is the reduced mass of an ion (m) and the neutral drift gas (M), and k is Boltzmann's constant.

3. Results and discussion

3.1. Effect of temperature on electrosprayed solvent ions

The solvent ions were monitored at different drift tube temperatures in order to determine any changes in the ESI process. Also, by monitoring the solvent ions as the drift tube temperature was increased, any deleterious effects on drift tube cleanliness could be observed. The predominant ions observed in the mass spectra for 5 temperatures (50 °C to 250 °C) are listed in Table 1. Several observations based on the predominant ions were made. First, at the lower temperatures (50 °C and 100 °C), water clusters were the predominating ions with $(H_2O)_3H^+$ (*m/z* 55) being the largest ion. Based on previous IMS literature, the stability of water clusters at low temperatures would be expected [30]. As the temperature was increased to 150 °C, the observed solvent ions changed. Of the previous ions, only the *m/z* 37 $(H_2O)_2H^+$ water cluster was observed. Also, ions with *m/z* values of 61, 83, 103, 121, and 146 were now seen. The ions (*m/z* 61, 83, and 103) were probably a result of gas phase reactions due to the acetic acid in the ESI solution. However, the two larger ions (*m/z* 121 and 146) were not typical solvent ions and were suspected to be

background air contaminants that had been deposited on the drift tube walls. Even at 150 °C, the effect of contaminants due to operating at lower temperature was seen. Spectrometer contamination could be one possible drawback of low temperature operation. The further increase in temperature to 200 °C showed an increase in the *m/z* 146 ion as well as the presence of a new ion, *m/z* 192, which was also thought to be a contaminant. At a drift tube temperature of 200 °C, there were no solvent ions observed and the two contaminants (*m/z* 146 and 192) dominated the mass spectrum. One benefit of high temperature operation is the volatilization of background contaminants and cleaning of the drift tube walls. Evaluation of the ions in Table 1 at 200 °C and 250 °C showed a decrease in the relative intensities of the two major contaminants at the higher drift tube temperature (250 °C).

In addition to MS, IMS spectra provide information on the ESI ionization efficiency and on desolvation of the ions. If desolvation were occurring within the drift region (after passing the gate), this would be experimentally observed as a decrease in resolution. The ion distribution will be changing throughout the IMS tube and the measured peak will broaden. In Fig. 1, the IMS solvent spectra were shown at the temperatures studied. In the lower temperatures (30 °C to 125 °C), the solvent peaks were broad, indicating incomplete desolvation. However, as the temperature was further increased, the peaks were better resolved. Until 150 °C, the IMS solvent spectra appeared similar to those observed at 125 °C, although the drift times were shorter due to increasing ion velocity with increasing temperature. The largest observed ion intensities were the fastest drifting ions with some smaller ions observed following the primary peak. These results were consistent with the mass spectral results, showing that the primary solvent peaks were composed of mainly water clusters (low *m/z* values). However, at 200 °C, there were two main IMS peaks (~20 and 24 ms), which corresponded to the two mass identified contaminants (*m/z* 146 and 192, respectively). At 250 °C, the contaminant peak intensity (now drifting at 22 ms) was reduced and solvent peaks were observed (similar to the trends in the mass-identified ions). Previous studies with our high resolution IMS/MS prior to the recent modifications found that complete desolvation of the solvent peaks was not obtained until 250 °C [14]. In comparison, these initial studies appeared to find that the solvent spectra were desolvated at 150 °C.

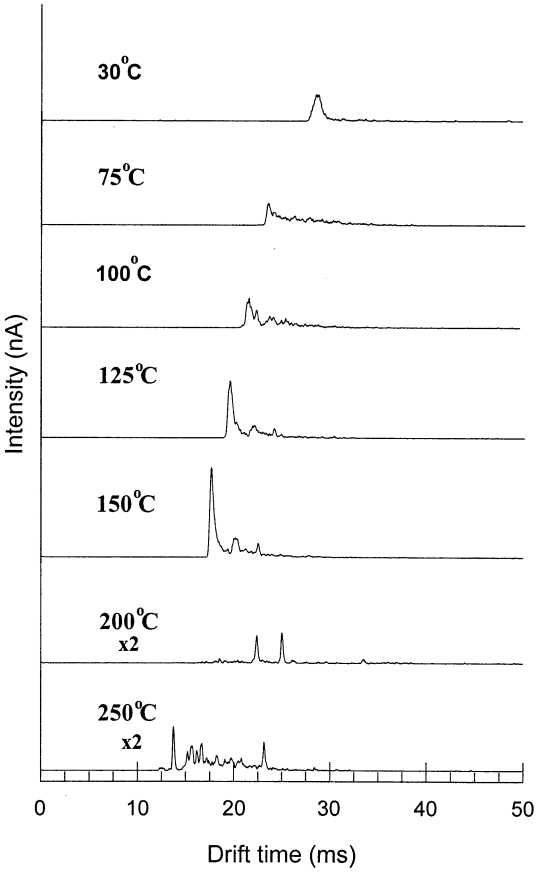

Fig. 1. Solvent spectra at different drift tube temperatures. Conditions: 100 μm i.d. capillary, 1 μl/min flow rate, mass spectrometer was operated in transmission mode allowing all ions to be detected.

3.2. Effect of electrospray flow rate on sensitivity and resolution

Typically with our system, a 100 μm i.d. capillary has been employed with a flow rate of 5 μL/min. For the following experiments, these two parameters were considered a base for which to compare results. Based on a theoretical model by Wilm and Mann [28], it was

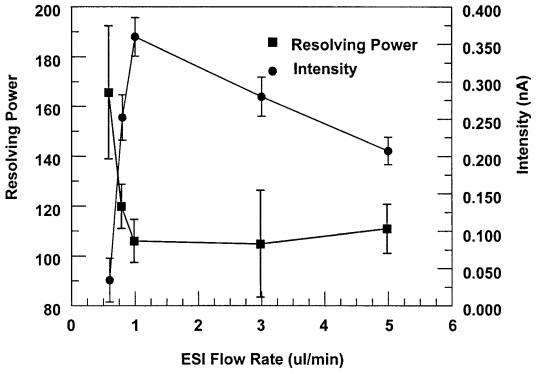

Fig. 2. Effect of ESI flow rate on signal intensity and resolving power. Conditions: 100 μm capillary i.d. and 125 °C.

shown that the size of droplets emitted from the Taylor cone was proportional to approximately two thirds the flow rate. Throughout the temperature and capillary studies, the flow rate was varied from 5 μL/min to 600 nl/min. A decrease in the droplet size could have two effects on the IMS results. First, the ionization efficiency would be increased due to a higher surface area on the droplet and hence more ions could be transferred to the gas phase. This effect would be realized by an increase in analyte intensity. The second effect would be less solvent molecules per droplet and consequently, the ions would require less energy or time to be completely desolvated. This would result in an increase in resolution at lower drift tube temperatures.

The effect of flow rate on both signal intensity (circle) and resolution (square) was shown in Fig. 2 (100 μm i.d. capillary, 125 °C). First, by evaluating the intensity, the maximal intensity was achieved at 1 μL/min. However, below this flow rate, the intensity steadily decreased and below 600 nl/min, the peptide signal was not observed. The initial increase in intensity with decreasing flow rate indicated that the ionization efficiency increased. Ionization efficiency is defined as the number of analyte molecules ionized over the number of analyte molecules sprayed [28]. Based on Fig. 2, a decrease in flow rate seemed to increase the ionization efficiency but there was a limit to where the decrease in flow rate did not compromise sensitivity. Because the droplets are smaller at low flow rates, there are less analyte molecules within each droplet. Therefore, once the efficiency was optimized, lower flow rates resulted in lower analyte signal intensity and this effect was attributed to the intensity decrease at flow rates below 1 μL/min. The second benefit of smaller droplets would be observed as an increase in resolution. In Fig. 2, the resolving power (plotted as the squares in the figure) remained unchanged until flow rates lower than 1 μL/min. The increasing resolving power after this point is thought to be due to the decrease in analyte ions rather than an effect of droplet size. A concentration dependence on resolving power possibly due to Coulombic repulsion between the ions has been observed previously [14]. Therefore, the flow rate was found to increase the ionization efficiency while showing little effect on the resolution. Variation in the flow rate was performed for all of the drift tube temperatures studied and similar results were obtained in all cases.

3.3. Temperature effect on IMS resolution and sensitivity

Previous studies on our IMS instrument have shown that drift tube temperatures below 150 °C caused decreased peak resolution due to incomplete desolvation [10]. Since these studies, the electric field in the desolvation region has been reduced to half of the drift region electric field. This change was performed to provide two benefits; (1) more of the voltage can be utilized for the drift region (increased resolving power) and (2) the ions would spend more time in the desolvation region. In this study, two parameters were tested in the temperature studies. First, employing a 100 μm i.d. capillary provided similar conditions to the previous studies of our IMS/MS instrument. The only difference would be the increased time in the desolvation region. By increasing the time the droplets spend in the desolvation region, there would be more time for complete ion desolvation prior to entry in the drift region. Less thermal energy (drift tube temperature) would be required to desolvate the ions and the IMS could be operated at lower temperatures. As described previously, the further decrease in the capillary diameter

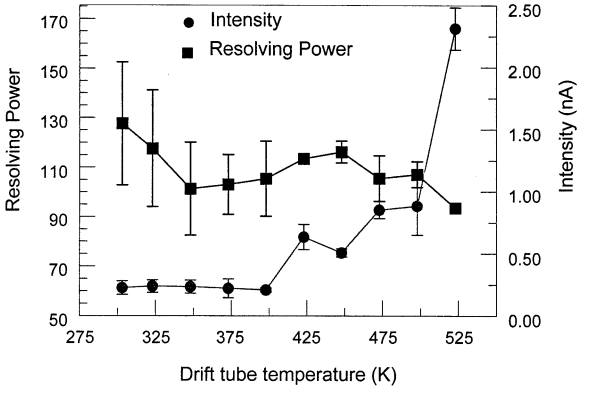

Fig. 3. Graph showing effect of drift tube temperature on both resolving power and intensity for typical ESI/IMS conditions: 100 μm i.d. capillary, 5 μL/min flow rate, and 1.1L/min drift gas.

should cause more efficient droplet formation and enable further decreases in temperature.

By decreasing the drift tube temperature, the peak broadening due to diffusion is decreased and the resolving power will increase [see Eq. (3)]. In Fig. 3, the effect of drift tube temperature on resolution (circles) was shown for the 100 μm i.d. capillary. Evaluation of the graph from the highest temperature (250 °C) to the lowest temperature (30 °C) showed that decreasing the temperature did increase the resolving power. Previous evaluations with our ESI/IMS/MS showed that there was an increase in resolution to 150 °C [10]. Below this temperature, the resolution decreased due to desolvation. In Fig. 3, a maximum resolution was reached at 150 °C and then the resolution decreased until 50 °C where the resolution greatly increased again. This feature has not been previously observed. Also in Fig. 3, as the drift tube temperature was decreased, the signal intensity (indicated by circles) decreased as well. This inverse relationship between signal intensity and IMS temperature has been observed in previous IMS systems [10] and is due to decreasing ion velocity, which results in increased ion collisions within the drift region. Thus, decreasing the drift tube temperature to improve the resolving power resulted in decreased instrumental sensitivity. Based on the initial experiments, it did not appear that increasing the time in the desolvation region caused a significant increase in the desolvation

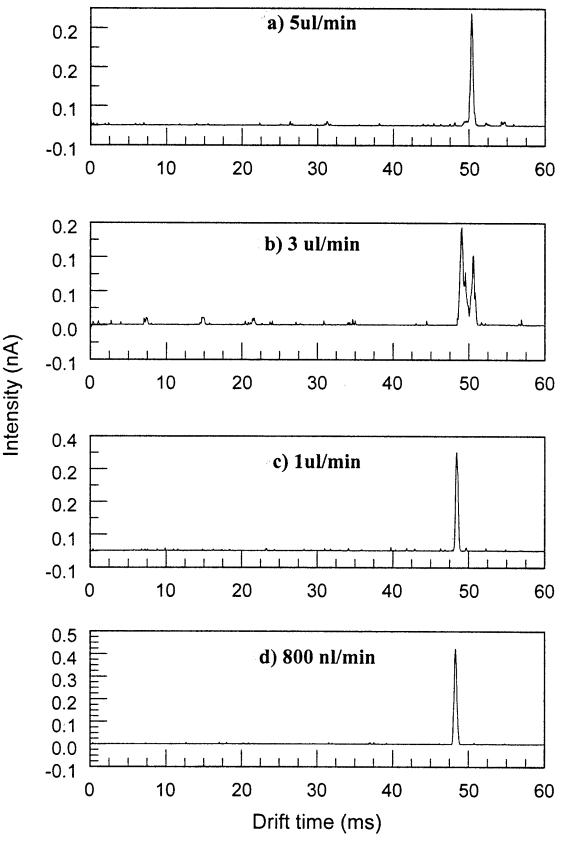

Fig. 4. Graph shows the change in ion mobility for GHK, a three amino acid peptide at 30 °C. Flow rates were as follows: (a) 5 μL/min,(b) 3 μL/min, (c)1 μL/min, and (d) 0.8 μL/min. Conditions: 30 °C, 100 μm i.d. capillary.

since the resolution for these experiments reached a maximum at 150 °C which was similar to previous studies [10]

Surprisingly, the resolution increased again at the low drift tube temperatures in Fig. 3. The mass-selected IMS spectra for GHK were shown in Fig. 4 at 4 flow rates. By comparing the four spectra, there were two distinct ion populations observed; the first at ~50 ms seen in **a** and **b** and a second at ~49 ms seen in **b**, **c**, and **d**. Since these ions were mass selected, the two ion populations had the same *m/z* value (mass resolution of the MS was ±1.5 amu). The drift time was observed to decrease as the flow rate was decreased from 5 μL/min (a) to 1 μL/min (c). One possible explanation for the change in drift time was

that the longer drifting ion seen in Fig. 4(a) contained a water molecule. Comparison of K_o values for the two ion populations (0.870 $cm^2V^{-1}s^{-1}$, 50 ms and 0.900 $cm^2V^{-1}s^{-1}$, 49 ms) with the smaller capillary diameter K_o values showed that the faster drifting ions had a similar K_o values to the ion mobilities of all flow rates with both of the smaller inner diameter capillaries. By decreasing the flow rate and consequently, the droplet size, the analyte ion was suspected to have lost the excess water molecules. It should be noted that all the ions had the same *m/z* value and the change could not be mass identified. However, this was not surprising considering that upon entering the vacuum region of the MS, most water molecules could be removed from ions. This change in ions would explain the shift in resolving power trends observed in Fig. 3. A decrease in resolving power due to incomplete desolvation was observed because ions were losing water molecules and changing size while transcending through the drift region. Differences in the ion population cased the ions to have different velocities and peak broadening was observed in the IMS spectra. However, at the lower temperatures and higher flow rates, the ions did not have enough energy to lose the excess water molecules and were therefore, observed as the longer drifting ion populations. At the lower flow rates, excellent resolution was obtained even with the larger capillary. In Fig. 4(c), a resolution of 120 was measured, which was a significant improvement over other attempts to operate at temperatures approaching room temperature [10].

Further evaluation of drift tube temperature effect was shown in Fig. 5 for all three capillary diameters. A better way to understand the relationship between temperature and resolution is to compare experimentally measured resolution with predicted resolution values. By comparison of the two values, any significant differences in resolution can be attributed to desolvation processes. The theoretical resolution has been plotted as well to show the theoretical effect of temperature and the points were calculated according to Eq. (3). First, the base example of 100 μm capillary i.d. was evaluated [shown in Fig. 5(a)]. In general, it can be seen that the theoretical resolution and average

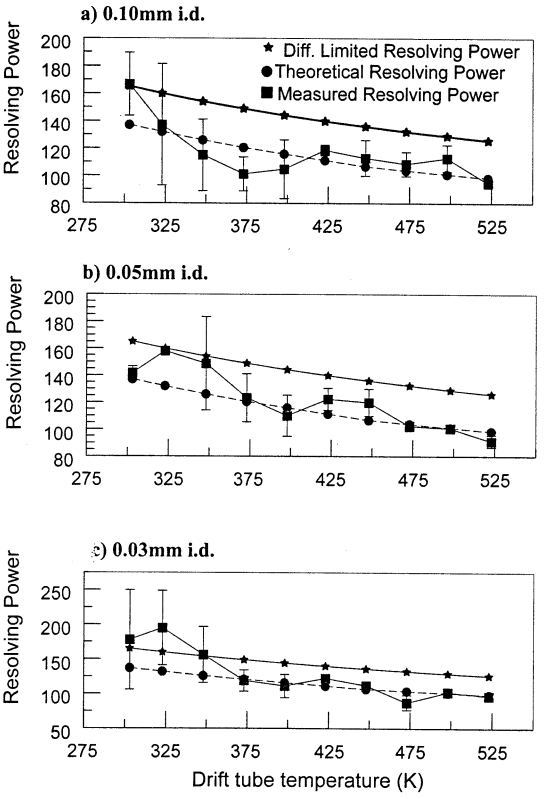

Fig. 5. Graph showing effect of drift tube temperature on resolving power for three different size capillaries. Values are compared with theoretical resolving power that was calculated base.

experimental resolution are approximately the same and follow a similar trend. However, as shown in Fig.3, the resolution decreased from 125 °C to 75 °C.

Evaluation of Fig. 5(b) and 5(c) showed that as the capillary size was decreased, the experimental and theoretical resolution began to converge to one line even at lower temperatures. This was a strong indication that the capillary diameter had an effect on the amount of desolvation required at lower temperatures and caused an improvement in the percent resolving power, which was achieved.

3.4. Desolvation of cytochrome C

Throughout the history of ESI/IMS development, the desolvation of small analyte molecules in atmospheric pressure drift tubes was found to be much

easier than for larger proteins [6,9]. The second evaluation employed cytochrome c to determine the optimal drift tube temperature for the IMS analysis of higher molecular weight molecules. The protein, cytochrome c, was chosen due to the abundance of studies that have characterized the conformers in reduced pressure drift tubes [13c,31,32]. The presence of multiple conformers for cytochrome c charge states have been observed and changes in temperature [13c] and increases in injection energies [32a] have been found to shift the measured collision cross sections. The collision cross sections obtained in these studies are not directly comparable to the work presented in this paper due to differences in instrumental setup and drift gas (reduced pressure systems commonly employ helium as the drift gas). However, it would be expected that multiple conformers for a charge state would also be measured in our IMS tube if the collision cross sections for the conformers were sufficiently different.

In Fig. 6, the nonselective IMS spectra for cytochrome c are shown for IMS studies employing the 100 μm i.d. capillary (a–c) and the 30 μm i.d. capillary (d–f) at three different temperatures; 100 °C (a and d), 150 °C (b and e), 200 °C (c and f). All other ESI conditions were the same for the spectra and the spectra shown were the result of 5000 averages. Due to the large number of averages, all peaks were thought to represent real ions. Looking at the three spectra for the 100 μm i.d. capillary, the highest resolution between the charge states was obtained at 150 °C (part b). This is concluded based on the overlap that is shown between the ion mobility peaks for each cytochrome c charge state. At both 100 °C and 200 °C (parts a and c), one predominant mobility peak is evident for each charge state. However, the nonselective IMS spectra at 150 °C included many shoulders on the mobility peaks for many of the charge states.

Comparison of the two sets of spectra in Fig. 6(a–c, 100 μm i.d.) and (d–f, 30 μm i.d.) showed that similar resolution results were obtained for the 30μm i.d. capillary where 150 °C was found to provide the optimum resolution for cytochrome c. Comparison of part b (100 μm i.d.) and part e (30 μm i.d.) elucidated

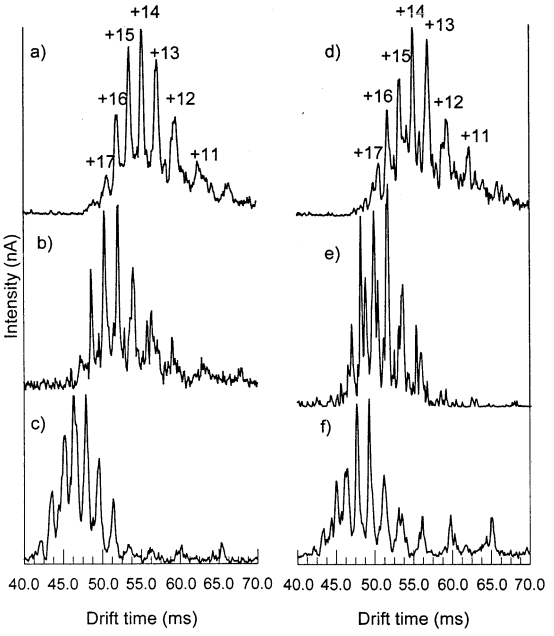

Fig. 6. Graph shows microspray/IMS spectra of cytochrome C at three different temperatures; (a) and (d) 100 °C, (b) and (e)150 °C, and (c) and (f) 200 °C. Conditions: (a)–(c) 100 μm i.d capillary and (d)–(f) 30 μm i.d. capillary, nonselective IMS mode (MS excluded ions with *m/z* values less than 700).

improvements in resolution based on capillary internal diameter and greater resolution between the shoulders observed in part b.

In Fig. 7, mass-identified mobilities are shown for four cytochrome c charge states (+13 to +16) under the same conditions as Fig. 6(e). The mass-selective mobilities confirmed that each shoulder peak was a conformer(s) from the assigned charge state. Although, there was overlap between the +13 and +14 charge state, the predominant peaks for each charge state had significantly different drift times and confirm the charge state identification presented for the nonselective IMS spectra in Fig. 6(e).

In Fig. 8, the collision cross sections were plotted for the major ions measured for cytochrome c with the 100 μm i.d. (closed circles) and the 30 μm i.d. capillary (open diamonds) at 150 °C. The graph shows that the collision cross sections for the two ion populations observed with the smaller capillary were similar in size to the single peaks measured with the

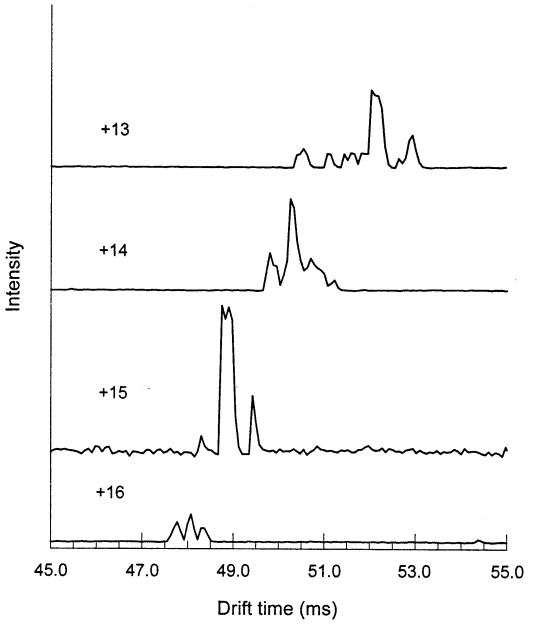

Fig. 7. Mass-selected ion mobility spectra for four cytochrome c charge states. Graph provides identification of predominant mobility peaks based on *m/z* for the specific charge state. Conditions: [similar to Fig. 6(e)] 150 °C, 30 μm i.d. capillary, 2 μL/min flow rate, 2000 averages for each mobility spectra.

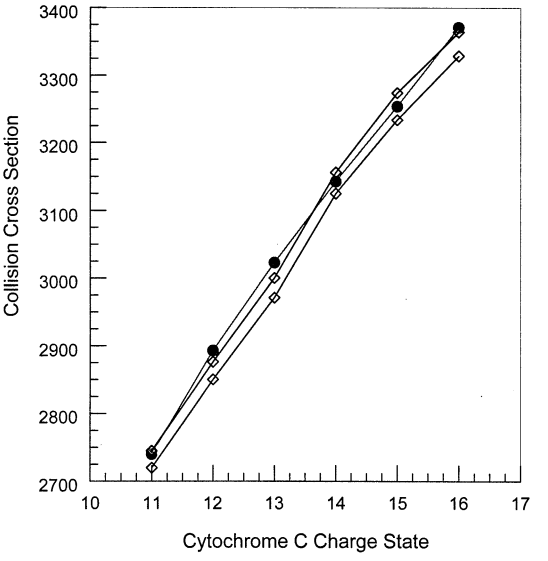

Fig. 8. Comparison of collision cross section for charge states ranging from +11 to +16 with 100 μm i.d. capillary (circles) and 30 μm i.d. capillary (open diamonds). Graph shows that two peaks were observed with the 30 μm i.d. capillary and that the measured collision cross sections are similar to the collision cross sections of the single peaks observed with the 100 μm i.d. capillary. Conditions: 150 °C, 5 μL/min ESI flow rate, MS was operated to transmit all ions greater than 600 amu.

100 μm i.d. capillary. The majority of the collision cross sections for the small capillary surrounded the collision cross sections measured for the larger capillary, providing further evidence that the two ion populations were observed as one broadened peak with the larger capillary.

4. Conclusions

Microelectrospray conditions were tested on our high resolution IMS/MS and found to improve the instrumental operation at lower temperatures. For smaller analytes, the analysis employing the smaller capillary diameter showed resolution values similar to theoretical at temperatures near ambient. This was a significant improvement over previous studies that found 150 °C to be the minimum allowable operating temperature without sacrificing resolution.

A second result of this work was the separation of cytochrome c charge states at lower temperatures. By employing the smaller capillary diameter, a higher resolving power was obtained and the presence of at least two distinct conformations were evident at 150 °C. Many protein conformer studies have been performed in low-pressure drift tubes and correlated with molecular dynamics simulations [32c]. Direct comparison between the collision cross sections measured with the current instrument and reduced pressure drift tubes would provide an understanding of the conformer structure(s), which were measured in this study.

Acknowledgements

This material is based upon work supported by the National Science Foundation under Grant 9870850. Any opinions, findings, and conclusions or recommendations expressed in this material are those of the authors and do not necessarily reflect the views of the National Science Foundation. This work was also

supported by the National Institutes of Health (Grant 8RO3DA1192302). The authors would like to acknowledge the support provided by the National Institute of Health for the National Research Scholarship Award for L.M. Matz.

References

[1] G.A. Eiceman, Z. Karpas, Ion Mobility Spectrometry, CRC Press, Boca Raton, FL, 1994.
[2] J. Gieniec, H.L. Fox, D. Teer, M. Dole, Abstracts 20th ASMS Conference on Mass Spectrometry Allied Topics, Washington, D.C., 1972, p. 267.
[3] M. Dole, C.V. Gupta, L.L. Mack, K. Nakamae, Polym. Prepr., Am. Chem. Soc., Div. Polym. Chem. 18 (1977) 188.
[4] (a) C.B. Shumate, H.H. Hill, Jr., Northwest Regional ACS Meeting, Bellingham, WA, June 1987. (b) C.B. Shumate, H.H. Hill, Jr., Anal. Chem. 61 (1989) 601.
[5] R.D. Smith, J.A. Loo, R.R. Ogorzalek, M. Busman, Mass Spectrom. Rev. 10 (1991) 359.
[6] D.P. Wittmer, Y.H. Chen, B.K. Luckenbill, H.H. Hill, Jr., Anal. Chem. 66 (1994) 2348.
[7] D.E. Clemmer, R.R. Hudgins, M.F. Jarrold, J. Am. Chem. Soc. 117 (1995) 10141.
[8] R. Guevremont, K.W.M. Siu, J. Wang, L. Ding, Anal. Chem. 69 (1997) 3959.
[9] (a) C. Wu, W.F. Siems, H.H. Hill, Jr., Anal. Chem. 72 (2000) 396. (b) M.A. McCooey, B. Ells, D.A. Barnett, P.W. Purves, R. Guevremont, J. Anal. Toxicol. 25 (2000) 81.
[10] G.R. Asbury, H.H. Hill, Jr., Int. J. Ion Mobility Spectrom. 2 (1999) 1.
[11] IMS of Tryptic Digests: (a) J.A. Taraszka, A.E. Counterman, D.E. Clemmer, Fresen. J. Anal. Chem. 359 (2001) 234. (b) S.J. Valentine, A.E. Counterman, D.E. Clemmer, J. Am. Soc. Mass Spectrom. 10 (1999) 1188. (c) S.J. Valentine, A.E. Counterman, D.E. Clemmer, J. Phys. Chem. 103 (1999) 1203. (d) R. Guevremont, D.A. Barnett, R.W. Purves, J. Vandermey, Anal. Chem. 72 (2000) 4577.
[12] IMS of Peptides: (a) R.W. Purves, D.A. Barnett, B. Ells, R. Guevremont, Rapid Commun. Mass Spectrom. 15 (2001) 1453. (b) T. Wyttenbach, G.von Helden, M.T. Bowers, J. Am. Chem. Soc. 118 (1996) 8355. (c) A.E. Counterman, A.E. Hildebrand, C.A. Srebalus-Barnes, D.E. Clemmer, J. Am. Soc. Mass Spectrom. 12 (2001) 1020. (d) C.A. Srebalus-Barnes, D.E. Clemmer, Anal. Chem. 73 (2001) 424. (e) J.A. Taraszka, J. Li, D.E. Clemmer, J. Phys. Chem. B 104 (2000) 4545. (f) T. Kaleta, M.F. Jarrold, J. Phys. Chem. B 105 (2001) 4436. (g) B.S. Kinnear, M.R. Hartings, M.F. Jarrold, J. Am. Chem. Soc. 123 (2001) 5660. (h) B.S. Kinnear, D.T. Kaleta, M. Kohtani, R.R. Hudgins, M.F. Jarrold, J. Am. Chem. Soc. 122 (2000) 9243.
[13] IMS of Proteins: (a) J. Li, J.A. Taraszka, A.E. Counterman, D.E. Clemmer, Int. J. Mass Spectrom. Ion Processes 185–187 (1999) 37. (b) Y. Mao, M.A. Ratner, M.F. Jarrold, J. Am. Chem. Soc. 122 (2000) 2950. (c) Y. Mao, J. Woenckhaus, J. Kolafa, M.A. Ratner, M.F. Jarrold, J. Am. Chem. Soc. 121 (1999) 2712. (d) R.W. Purves, D.A. Barnett, B. Ells, R. Guevremont, J. Am. Soc. Mass Spectrom. 12 (2001) 894. (e) R.W. Purves, D.A. Barnett, R. Guevremont, Int. J. Mass Spectrom. Ion Processes 197 (2000) 163.
[14] C. Wu, W.F. Siems, G.R. Asbury, H.H. Hill, Jr., Anal. Chem. 70 (1998) 4929.
[15] Reviews of IMS for Analysis of Proteins and Peptides: (a) D.E. Clemmer, M.F. Jarrold, J. Mass Spectrom. 32 (1997) 577. (b) C.S. Hoaglund-Hyzer, A.E. Counterman, D.E. Clemmer, Chem. Rev. 99 (1999) 3037. (c) Y. Liu, S.J. Valentine, A.E. Counterman, C.S. Hoaglund, D.E. Clemmer, J. Am. Chem. Soc. 69 (1997) 728A. (d) M.F. Jarrold, Ann. Rev. Phys. Chem, 51 (2000) 179.
[16] K. Shelimov, M.F. Jarrold, J. Am. Soc. Mass Spectrom. 118 (1996) 131.
[17] S.J. Valentine, J.G. Anderson, A.D. Ellington, D.E. Clemmer, J. Phys. Chem. B 101 (1997) 3891.
[18] W.F. Siems, C. Wu, E.E. Tarver, H.H. Hill, Jr., P.R. Larsen, D.G. McMinn, Anal. Chem. 66 (1994) 4195.
[19] G.R. Asbury, H.H. Hill, Jr., J. Microcol. Separations 12 (2000) 172.
[20] H.E. Revercomb, E.A. Mason, Anal. Chem. 47 (1975) 970.
[21] P.H. Dugourd, R.R. Hudgins, D.E. Clemmer, M.F. Jarrold, Rev. Sci. Instrum. 68 (1997) 1122.
[22] J.W. Leonhardt, W. Rohrbeck, H. Bensch, Fourth International IMS Workshop, Cambridge, UK, 1995.
[23] C.A. Srebalus, J. Li, W.S. Marshall, D.E. Clemmer, Anal. Chem. 71 (1999) 3918.
[24] D.C. Collins, M.L. Lee, Fresenius' J. Anal. Chem. 369 (2001) 225.
[25] R.M. Caprioli, M.E. Emmett, P. Andren, Proceedings of the 42nd ASMS Conference on Mass Spectrometry and Allied Topics, Chicago, IL, May 29–June 3 1994, p.754.
[26] R.M. Caprioli, M.E. Emmett, J. Am. Soc. Mass Spectrom. 5 (1994) 605.
[27] M. Wilm, M. Mann, Proceedings of the 42nd ASMS Conference on Mass Spectrometry and Allied Topics, Chicago, IL, May 29–June 3 1994, p. 770.
[28] M. Wilm, M. Mann, Anal. Chem. 68 (1996) 1.
[29] M.S. Wilm, M. Mann, Int. J. Mass Spectrom. Ion Processes136 (1994) 167.
[30] S.H. Kim, K.R. Betty, F.W. Karasek, Anal. Chem. 50 (1978) 2006.
[31] R.W. Purves, R. Guevremont, Anal. Chem. 71 (1999) 2346.
[32] (a) K.B. Shelimov, D.E. Clemmer, R.R. Hudgins, M.F. Jarrold, J. Am. Chem. Soc. 119 (1997) 2240. (b) S.J. Valentine, D.E. Clemmer, J. Am. Chem. Soc. 119 (1997) 3558. (c) Y. Mao, M.A. Ratner, M.F. Jarrold, J. Phys. Chem. B 103 (1999) 10017.